Twin-screw extrusion impact on natural fibre morphology and material properties in poly(lactic acid) based biocomposites

Guillaume Gamon, Philippe Evon, Luc Rigal

Twin-screw extrusion impact on natural fibre morphology and material properties in poly(lactic acid) based biocomposites

G. Gamon[a,b,*], Ph. Evon[a,b], L. Rigal[a,b]

[a] Université de Toulouse, INP, Laboratoire de Chimie Agro-industrielle, ENSIACET, 4 Allée Emile Monso, BP 44362, 31030 Toulouse Cedex 4, France
[b] INRA, Laboratoire de Chimie Agro-industrielle, 31030 Toulouse Cedex 4, France

Keywords:
Twin-screw extrusion
Biocomposite
Poly(lactic acid)
Natural fibre
Mechanical and thermal properties

A B S T R A C T

Natural fibres from miscanthus and bamboo were added to poly(lactic acid) by twin-screw extrusion. The influence of extruder screw speed and of total feeding rate was studied first on fibre morphology and then on mechanical and thermal properties of injected biocomposites. Increasing the screw speed from 100 to 300 rpm such as increasing the feeding rate in the same time up to 40 kg/h helped to preserve fibre length. Indeed, if shear rate was increased with higher screw speeds, residence time in the extruder and blend viscosity were reduced. However, such conditions doubled electrical energy spent by produced matter weight without significant effect on material properties.

The comparison of four bamboo grades with various fibre sizes enlightened that fibre breakages were more consequent when longer fibres were added in the extruder. Longer fibres were beneficial for material mechanical properties by increasing flexural strength, while short fibres restrained material deformation under heat by promoting crystallinity and hindering more chain mobility.

1. Introduction

Environmental concerns have led over the past years to growing research over new solutions for plastics. Work over "green plastics" have been motivated by two specific goals: reducing dependence of plastic production on petroleum supplies, that will decrease in the future, and developing solutions to plastic waste accumulation. The development of biobased and biodegradable polymers is a 'cradle to grave' approach aiming to use renewable resources and to limit waste.

Thermoplastic starch (TPS), polyhydroxyalkanoates (PHAs), polylactides and their blends are promising candidates for such replacement and are subject to many researches. Poly(lactic acid) (PLA) has been intensively investigated in past years. This biodegradable polyester, which can be used in many applications from packaging to biocompatible materials, has a thermoplastic behaviour combined with high mechanical performance, good appearance and low toxicity (Jamshidian et al., 2010).

Blending polyolefins and polyesters with natural fibres is a known way to reduce production costs while saving or increasing the matrix properties (Mohanty et al., 2000; Faruk et al., 2012). Natural fibres are renewable, and they have the advantages over glass or carbon fibres to be abundant and cheaper. Moreover, they have a high toughness–density ratio and good thermal properties on the insulation viewpoint. Kymäläinen and Sjöberg (2008) referenced the thermal conductivity of different flax and hemp fibre mats (from 33 to 94 mW/m K) and showed that it was comparable to thermal conductivities of glass wool (50 mW/m K and below) or stone wool (from 35 to 71 mW/m K). For comparison, NatureWorks LLC announced thermal conductivity of 160 mW/m K for its PLA grades. Despite these advantages, fibre hydrophilic behaviour can be a source of incompatibility with the matrix and can increase biocomposite moisture-sensitivity. PLA-based biocomposites have been widely studied and several types of vegetal fibres have been incorporated (Faruk et al., 2012). Fibres coming from wood (Huda et al., 2006; Sykacek et al., 2010), flax (Oksman et al., 2003), hemp (Masirek et al., 2007), kenaf (Ogbomo et al., 2009) and jute (Plackett, 2004) have been tested among others. Lezak et al. (2008) and Nyambo et al. (2010) also studied the incorporation of various agricultural residues. From these studies, it was revealed that the fibre type has a real importance on composite performance. They enlightened a lack of interactions between the PLA and the tested fibres resulting in a weak interface unable to transfer efficiently stress from the matrix to the reinforcing fibre during mechanical solicitation. This resulted in mechanical strength reduction without any chemical or physical compatibilisation made to enhance fibre–matrix interface.

Miscanthus (*Miscanthus giganteus*) and bamboo (*Thyrsostachys oliverii*) are two perennial crops characterized by high yields. Miscanthus is a rhizomatous grass related to sugarcane that originated

* Corresponding author at: Agromat, site de l'ENIT, 47 Avenue d'Azereix, BP 1629, 65016 Tarbes Cedex, France. Tel.: +33 5 62 44 60 84; fax: +33 5 62 44 60 82.
E-mail addresses: guillaume.gamon@ensiacet.fr (G. Gamon), philippe.evon@ensiacet.fr (Ph. Evon), luc.rigal@ensiacet.fr (L. Rigal).

from Southeast Asia, and was originally introduced into Europe as an ornamental garden grass (Johnson et al., 2005). Bamboo grows up to 40 m of height in monsoon climates. Generally, it is used in construction, carpentry, weaving and plaiting, etc. (Faruk et al., 2012). Both miscanthus and bamboo attracted attention for fuel production (Hong et al., 2011) but also for biocomposites reinforcement. Bourmaud and Pimbert (2008) tested, by nanoindentation, modulus and hardness of miscanthus fibre being 9.49 GPa and 0.34 GPa, respectively, showing it to have modulus between sisal (8.52 GPa) and hemp (12.14 GPa). They worked to incorporate miscanthus in PLA and polypropylene (PP) too, showing comparable performance to other fibres. Johnson et al. (2005) also worked to blend miscanthus with Mater-Bi® to improve its impact performance. Mater-Bi® had a 0.8 J puncture energy, tested by an instrumented falling dart impact tester, that was increased up to 1.9 J with miscanthus fibres. Okubo et al. (2004) compared bamboo fibre properties to those of jute fibres. Tested bamboo fibres had a 441 MPa tensile strength and a 35.9 GPa modulus, what was higher to jute fibres strength and modulus (370 MPa and 22.7 GPa, respectively). Bamboo was investigated with PLA by Tokoro et al. (2008). They proved that depending on the extraction method of bamboo fibres, these ones can reinforce or not material bending strength. Short bundles (215 μm in length and 39 μm in diameter) were less efficient than longer fibres from steam exploded pulp (1740 μm in length and 24 μm in diameter), and their respective strengths were around 80 MPa and 115 MPa. They also showed that 3 mm bamboo fibre bundles could improve PLA Izod impact strength from 1.5 to more than 5 kJ/m^2, while 0.2 mm bundles decreased it to 1 kJ/m^2.

The process used for biocomposite production has a high importance too. A good fibre dispersion is needed to aim good material performance. Fibre orientation will play a role since fibres reinforce more the material in their longitudinal direction (Joseph et al., 1999). In addition, many models on composites have enlightened the importance of fibre aspect ratio in mechanical properties, which is defined by the ratio between its length (L) and its diameter (d). According to them, keeping a high aspect ratio brings more stiffness to the biocomposite. Shear applied during the compounding and moulding processes will cause fibre breakages. However, natural fibres, often linked together by pectic substances into bundles, have the ability to get separated under shear, what reduces their final diameter. Joseph et al. (1999) showed that increasing rotor speed during PP-sisal melt-mixing caused more fibre breakage with a large increase of small length fraction in fibre size distribution. Also, less fibre breakage was observed when temperature was higher and so reduced blend viscosity. Le Duc et al. (2011) investigated flax fibre behaviour under shear in a rheo-optical system, observing several fibre bendings before rupture. They also observed a high loss in length after compounding in an internal mixer. Flax fibres with a 10 mm initial length were reduced to a 96 μm average length in number. Twin-screw extrusion is a high shear process that can help to match a good fibre dispersion. Bledzki et al. (2005) observed better mechanical properties by compounding PP and wood in a twin-screw extruder compared to high speed mixer and two-roll mill. Nevertheless, extrusion leads to several fibre breakages. Tokoro et al. (2008) have seen length reduction from 215 to 86.3 μm and diameter reduction from 39.2 to 21.3 μm for short bamboo fibre bundles, after extrusion and injection. Wollerdorfer and Bader (1998) observed this drastic shortening of fibres too, in the case of flax-based biodegradable polymer composites. They saw differences in fibre length distributions, due to the chosen matrix and its rheology. Indeed, distributions, after fibre addition in Bionolle® with low melt viscosity, were wider with long fibres than distributions for TPS or Biocell® biocomposites. By increasing the fibre content in TPS from 10 to 20%, they showed considerable increase of the fibre percentage in the lower length fraction under 200 μm. Beaugrand and Berzin (2012) correlated hemp fibre length reduction to the increasing specific mechanical energy (SME) spent during compounding by twin-screw extrusion in polycaprolactone (PCL) matrix. The couple barrel temperature and fibre moisture content was also found to have an importance. Fibre length and aspect ratio were more preserved with a 100 °C barrel temperature and a 22.5 wt% moisture in fibre, than with 140 °C and 9.8 wt% moisture. Two studies observed that fibre breakage and separation from bundle to elementary fibre would be more or less important depending on the fibre origin. First, Oksman et al. (2009) compared sisal, flax, banana and jute, and found that flax fibres obtained by enzymatic retting process and having low lignin content, are better separated than the others in natural fibre reinforced PP. In Le Moigne et al. (2011) study, flax fibres were also separated in elementary fibres while sisal fibres remained partly in bundles and wheat straw provided bundles and large amounts of small particles.

This study aimed to investigate the influence of the compounding parameters on natural fibre morphology, mechanical properties and thermal properties in poly(lactic acid) based biocomposites. For this, miscanthus fibres were compounded to a PLA commercial grade in a twin-screw extruder at different feeding rates and different screw speeds to control shear in the machine, and the miscanthus/poly(lactic acid) blends were then injected. The fibre size preservation depending on its initial size was also studied. For that, different calibrated grades of bamboo fibres were used and compared to miscanthus.

2. Materials and methods

2.1. Materials

Fibres are available commercial grades. Miscanthus fibres (MIS) were provided by Miscanthus Green Power (France), and bamboo fibres were provided by Bamboo Fibers Technology (France). Four different grades of bamboo fibres, named B1 to B4 from the longer to the shorter one, were used for this study. The chemical compositions and initial morphologies of the five fibres tested are reported in Table 1. SEM images of the different fibres before compounding, taken with a JEOL JSM-700F (Japan) scanning electron microscope, using a 5 kV accelerating voltage, are shown in Fig. 1. Fibres were vacuum-coated two times with palladium for observation to avoid charging under the electron beam. It can be seen that fibres were held together in bundles. Moreover, it was noticed that contrary to miscanthus bundles, bamboo bundles exhibited fibre separation at their end. The shorter bamboo grade B4 was composed of smaller bundles on which this fibre separation was less visible.

Poly(lactic acid) was a Natureworks LLC (USA) Ingeo™ grade, and it was supplied in the form of granules.

2.2. Fibre chemical composition

Characterization of the different fibre chemical compositions focused on lignocellulose, lipids, ash and hot water extractible compounds. Amounts of cellulose, hemicelluloses and lignins were determined according to the ADF-NDF technique (Van Soest and Wine, 1967, 1968). Lignins were oxidized by a potassium permanganate solution. Results obtained for miscanthus (Table 1) were close to those obtained by Van Hulle et al. (2010) with the same technique. Lipids were determined by Soxhlet extraction using cyclohexane as extracting solvent (French standard NF V 03-908). Samples were burnt off at 550 °C during 5 h for the ash content determination (French standard NF V 03-322). For the hot water extracts content determination, extraction was made by refluxing distilled water for 1 h. The hot water extracts can contain inorganic compounds, tannins, gums or sugars. All determinations were carried out in duplicate.

Table 1
Chemical composition and initial morphology of the different fibres tested.

	Miscanthus (MIS)	Bamboo (B1)	Bamboo (B2)	Bamboo (B3)	Bamboo (B4)
Chemical composition (wt% of the dry matter)					
Cellulose	61.1 (0.4)	65.5 (1.4)	66.1 (1.3)	60.2 (1.8)	43.6 (1.2)
Hemicelluloses	23.3 (1.0)	12.3 (2.0)	11.0 (1.4)	13.3 (1.5)	17.4 (0.8)
Lignins	6.8 (0.6)	14.5 (0.4)	14.3 (0.6)	17.6 (0.9)	21.0 (0.5)
Lipids	0.8 (0.0)	0.2 (0.1)	0.2 (0.1)	0.1 (0.0)	0.3 (0.1)
Ash	1.7 (0.1)	1.9 (0.1)	1.2 (0.0)	2.1 (0.0)	3.4 (0.0)
Hot water extracts	5.3 (0.3)	5.8 (0.8)	6.8 (1.5)	6.1 (0.3)	12.8 (0.5)
Fibre morphology					
Mean length (mm)	1.69 (0.85)	3.24 (1.68)	2.12 (0.83)	1.29 (0.76)	0.49 (0.26)
Mean diameter (mm)	0.23 (0.14)	0.26 (0.20)	0.20 (0.10)	0.16 (0.10)	0.08 (0.04)
Mean aspect ratio	8.6 (5.0)	17.2 (11.1)	13.0 (7.3)	9.6 (6.6)	8.6 (7.2)

Numbers in parentheses correspond to the standard deviations.

2.3. Compounding

Prior to extrusion, fibres have been dried overnight at 80 °C. After drying, 3–4 wt% remaining moisture in the fibres was measured according to the French standard NF EN ISO 665. Compounding was carried out in a co-rotating twin-screw extruder with a 44 L/d ratio and a 28.3 mm screw diameter. It consisted in 11 successive modules. PLA was fed in module 1 of the extruder and the fibre introduction was made through a side feeder in module 6 after PLA melting. Three distinct zones made of kneading elements were located in modules 7–9 to disperse fibres in the melted PLA. Temperature was set at 190 °C in the melting zone, and at 165 °C in the kneading zone. Four different screw speeds (n) were tested during the study: 100, 150, 225 and 300 rpm, with 20 kg/h in total feeding rate (Q), i.e. PLA plus natural fibres. Q/n ratios were 0.20, 0.13, 0.09 and 0.07 kg/h/rpm, respectively. In addition, compounding was carried out at these four different screw speeds for a 0.13 kg/h/rpm Q/n ratio, corresponding to feeding rates of 13, 20, 30 and 40 kg/h, respectively. Matter pressure (P_{mat}, bars) and temperature in the die as well as test torque (T, %) of the extruder motor have been measured with specific detectors, and recorded every minute during production. The resulting specific mechanical energy (SME, (W h)/kg) was calculated with the following equation:

$$\mathrm{SME} = \frac{P_M \times (T/T_{max}) \times (n/n_{max})}{Q}.$$

P_M (41 W) is the motor's electric power, T_{max} (100%) is the maximum torque of the extruder motor, and n_{max} (1200 rpm) is the maximum speed of the rotating screws. The SME corresponds to the electrical energy consumed by the motor per weight unit of matter to ensure the compounding.

Compound rods were cooled with water and air, and then were pelletized. Pellet length was around 3.61 ± 0.26 mm (mean value obtained after the length measurement of 20 pellets using an electronic digital sliding calliper having a 0.01 mm resolution).

2.4. Injection moulding

An injection press with 150 tonnes clamping force was used to make standard dumbbell shaped samples for mechanical property measurements. Pellets were dried at 60 °C during 4 h prior to moulding. Temperature profile along the plasticating screw was 30–155–160–165–165 °C and the die temperature was 170 °C. Screw speed for melting was set at 150 rpm and injection speed was set at 50 mm/s. The mould was kept at 18 °C with water circulation.

2.5. Rheological measurements

Relative viscosity measurements have been carried out on extruded pellets in a Thermo Haake (Germany) MiniLab micro compounder. It consists in a co-rotating twin-screws configuration. The MiniLab is equipped with a backflow channel designed as a slit capillary. Pressure is measured at the capillary entrance and exit. Shear stress is deduced from the pressure drop in the back flow channel during melt polymer recirculation. Different relative shear rates were studied by changing screw speed. Measurements have been made at 170 °C with screw speeds from 50 to 250 rpm corresponding to relative shear rates between 177 and 889 s^{-1}. Measured viscosities and shear rates are called "relative" in the case of MiniLab measurements, as volumic flow is not set but estimated thanks to the screw speed. Slip effects along the device wall could also cause deviation from absolute viscosity values, as stated on the device's technical documentation. To avoid any interference of residence time in our comparisons, a time gap of 1.5 min between each measurement was set. All determinations were carried out in duplicate.

2.6. Fibre extraction and fibre size measurements

Fibres were extracted from biocomposites by dissolving PLA in chloroform using a Soxhlet extraction apparatus. Fibre pictures were taken with a Nachet (France) Rubis binocular magnifier with a 5.5×–10× observing magnification depending on the fibre size. An image was taken for each analysed sample using the Archimed 4.0 (France) software. The picture resolution was 14 and 7 μm/pixel, respectively, what was a good resolution to have a sufficient number of fibres to characterize on the picture and to observe various bundle sizes. However, this method was limited for measuring elementary fibres. Due to picture resolution, measurements of specimen under 30 μm were difficult. Length and diameter were manually measured with the ImageJ (USA) software. 200 fibres by sample were measured in order to set length, diameter and aspect ratio distributions. Care has been taken to label fibres measured to avoid duplicates. In order to compare the samples, size distributions were built and superposed. In this paper, mean values of length, diameter and aspect ratio are presented, to clearly represent observations made on the size distributions. They were calculated in number.

2.7. Mechanical testing

Tensile and flexural properties were measured using a Tinius Olsen (USA) universal testing machine fitted with a 5 kN load cell according to the French standards NF EN ISO 527 and 178, respectively. The crosshead speed for tensile testing was 5 mm/min and tensile modulus was determined with an extensometer at the speed of 1 mm/min. The crosshead speed for the three-point bending flexural test was 2 mm/min for a 64 mm gap. Samples were stored for two weeks in a climatic chamber set at 25 °C and 60% relative humidity before testing. Six samples per testing mode were analysed.

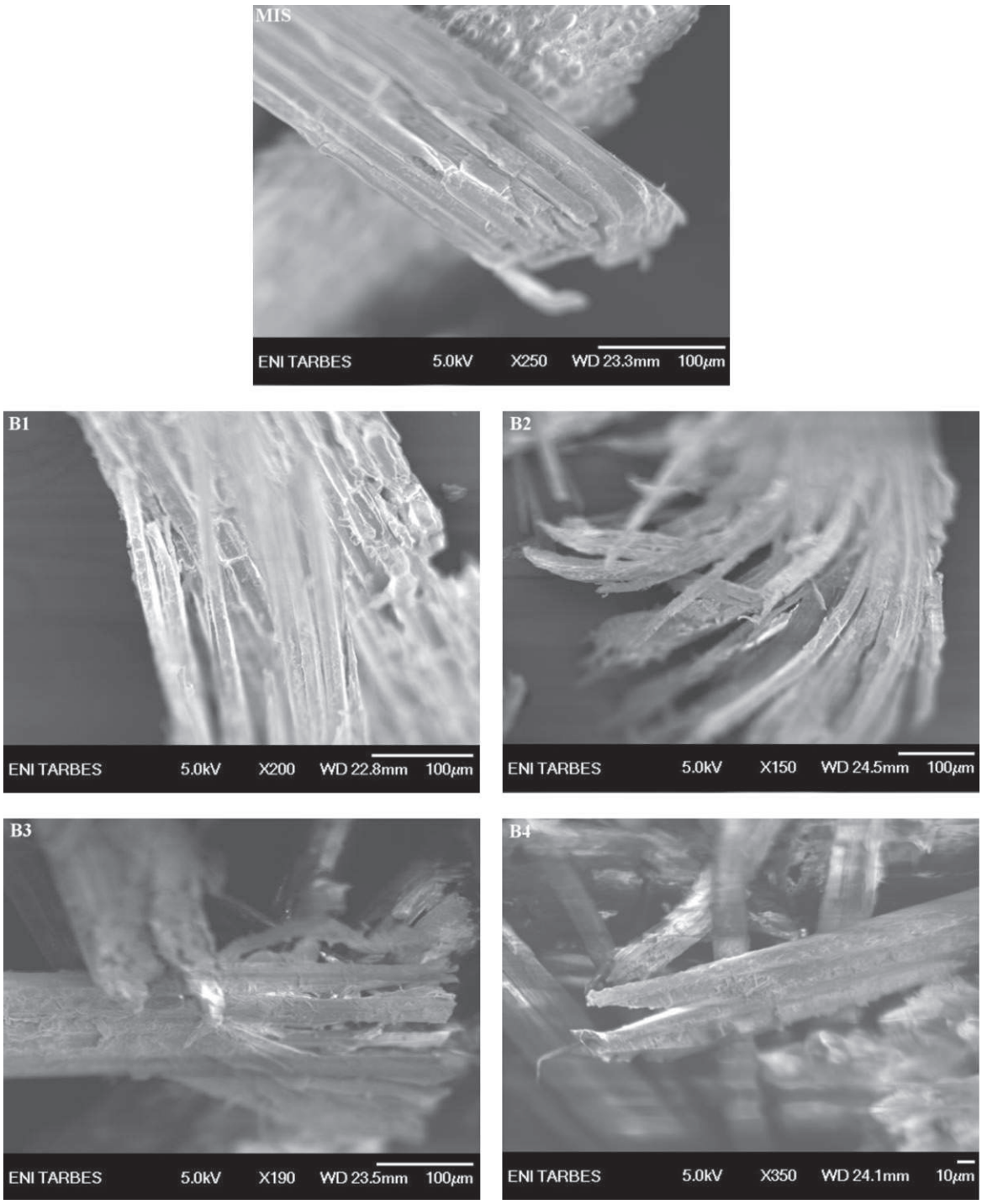

Fig. 1. SEM images of miscanthus fibres (MIS) and bamboo fibre grades (B1 to B4) before compounding.

2.8. Differential scanning calorimetry (DSC)

PLA transition temperatures were determined using a Mettler Toledo (Switzerland) DSC821^e calorimeter under nitrogen flow. Samples for DSC analysis were obtained from injected composites after a two-week storage in a climatic chamber set at 25 °C and 60% relative humidity. A first heating ramp at 10 °C/min until 200 °C was performed to erase sample thermal history. After a cooling ramp until 25 °C at 15 °C/min and 10 min isotherm at 25 °C to end the cooling, a second heating in the same conditions was carried out. Two analyses were made by sample. The glass transition (T_g), cold crystallization (T_{cc}), and melting (T_m) temperatures were determined from the last heating ramp. T_g was taken as the midpoint of the DSC curve deflection from baseline. Enthalpy values were determined using STAR^e SW 9.30 software from Mettler-Toledo by integrating the area of the cold crystallization and melting peaks and doing the ratio between the measured area and the real PLA mass in the biocomposite. Crystallinity rate (χ) after cooling step was calculated as following:

$$\chi = \frac{\Delta H_f - \Delta H_{cc}}{\Delta H_{fth}},$$

where ΔH_f is the sample melting enthalpy (J/g), ΔH_{cc} is the sample cold crystallization enthalpy (J/g) and ΔH_{fth} the theoretical melting enthalpy for 100% crystalline PLA taken to be 93.6 J/g (Fischer et al., 1973; Tuominen et al., 2002). Variations in used values for this theoretical melting enthalpy could be found ranging from 93 to 93.7 J/g in two of the previously reported works (Tokoro et al., 2008; Nyambo et al., 2010).

2.9. Dynamic mechanical analysis (DMA)

Dynamic mechanical properties, i.e. storage modulus, loss modulus and loss factor ($\tan\delta$), defined as the ratio of the loss modulus to the storage one, were determined using a Triton Technology (UK) TTDMA device. Tests were performed using single cantilever geometry over samples with 25 mm length, 10 mm width and 4 mm thickness. Distance between clamps was 10 mm. Strain of 1 Hz frequency and 20 μm amplitude was used. Heating ramp from ambient temperature to 160 °C was carried out at a rate of 2 °C/min. Analyses were performed on injected samples stored at least two weeks in controlled conditions (25 °C; 60% RH) and were duplicated to confirm the repeatability.

2.10. Heat deformation

Deformation of PLA injected objects could limit their usage in thermally processed packages for instance (Jamshidian et al., 2010). The non-normalized test proposed here is a comparative study of heat stabilities for PLA and PLA biocomposites. Dimensional stability of injected pieces was determined on standard dumbbell shaped samples after storage in an oven at 80 °C during 1 h. Such temperature was chosen to be higher than PLA glass transition temperature, and lower than cold crystallization and melting ones. Pieces were hold by a grip on one side, the other side being let free in the air. After the heat treatment, the sample bend by its free side and angle variation between the two sides could be then determined (Fig. 2). This variation was measured on a side view picture of the sample with the ImageJ software. Two samples were heat-treated by lot, after a storage of at least two weeks in controlled conditions (25 °C; 60% RH). The heat deformation of PLA biocomposites (%) was then defined as the ratio between the angle variation and the initial horizontal angle (180°). In this non-normalized test, no force was applied to the sample, except its own weight and possibly air flow in the oven. Consequently, the results presented in this study can be considered as a first clue of shape deformation improvement but do not represent heat stability under load as the test determining the heat deflection temperature (HDT) can do (standard ASTM D648).

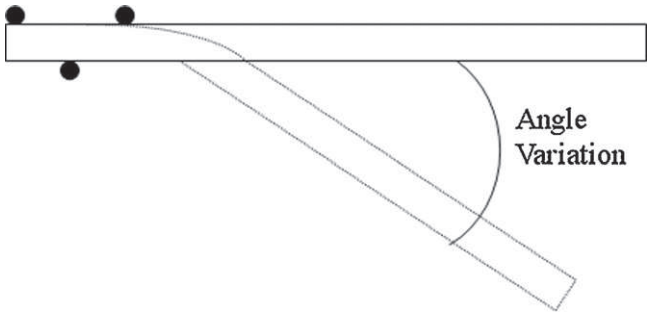

Fig. 2. Representation of sample bending and deformation angle, black circles representing the grip holding the sample on one side.

2.11. Size-exclusion chromatography (SEC)

A Dionex (France) size exclusion chromatography equipped with a Iota2 refractive index (RI) detector was used to determine PLA molecular weight distribution in the injected material. Three PLgel columns were associated in series of 10^3, 500 and 100 Å along with a precolumn. Columns were kept at a 30 °C temperature. PLA separated from fibres, during previous Soxhlet extraction in chloroform, was used for characterization. PLA was removed from extracting chloroform by evaporation. It was then dissolved again in clear chloroform at an approximate 5 mg/mL concentration. Chloroform was also used as eluent for the analyses. Polystyrene standards were used for the calibration. Soxhlet extraction was compared to PLA extraction by simple dissolution in chloroform at ambient temperature followed by Buchner filtration to remove fibres and solvent evaporation. No differences were observed in PLA molecular weight distributions.

3. Results and discussion

3.1. Composites processing

During extrusion, torque evolution was measured in order to compare the extruder force needed to convey and to mix the two raw materials, i.e. PLA and natural fibres. From the torque value, the SME value was deduced, representing the specific mechanical energy (per weight unit of matter) spent to compound the fibres with PLA. Passing through the die was also an important step during extrusion process. As a response of compound state into the die, the matter pressure was controlled. This parameter could be influenced by many variables such as the die geometry, its filling degree, the temperature or the compound viscosity.

Table 2
Extrusion parameters for various fibre types and loadings with a 150 rpm screw speed.

Fibre type	Fibre loading (wt%)	Q (kg/h)	T (%)	P_{mat} (bars)	SME ((W h)/kg)
Without fibre	0	20	46 (0.0)	18 (0.1)	118
MIS	10	20	51 (0.6)	27 (0.6)	130
	20	20	57 (0.7)	34 (0.6)	145
	40	20	67 (0.9)	56 (1.9)	170
B1	20	20	51 (0.5)	28 (0.5)	131
	40	15	41 (1.0)	44 (1.2)	140
B2	20	20	53 (0.7)	29 (0.5)	136
	40	12	43 (0.8)	35 (1.3)	184
B3	20	20	52 (0.7)	31 (0.5)	133
	40	20	65 (0.9)	55 (1.7)	167
B4	20	20	53 (0.6)	34 (0.7)	136
	40	20	68 (4.0)	73 (5.3)	174

Numbers in parentheses correspond to the standard deviations.

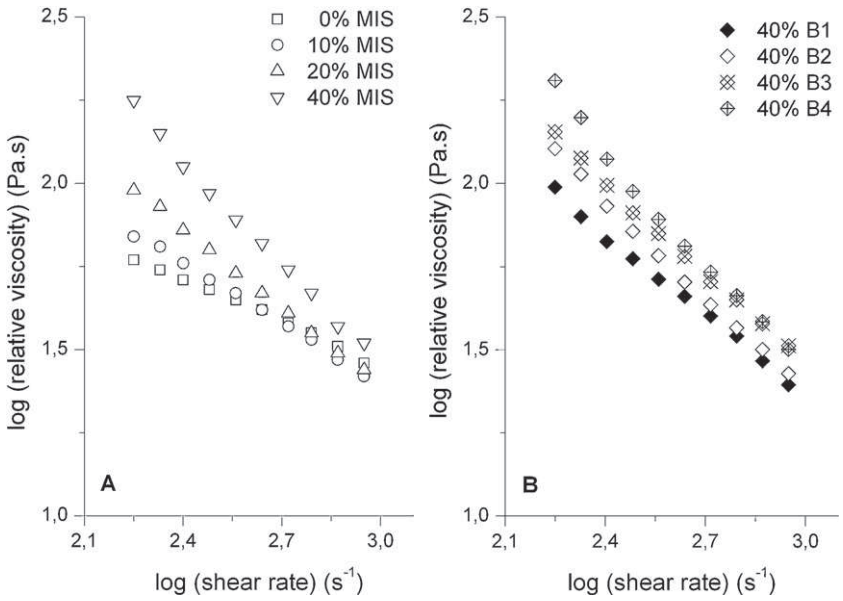

Fig. 3. MiniLab relative rheological measurements (A) for PLA-miscanthus composites with increasing fibre contents from 0 to 40 wt% and (B) for 60/40 PLA–bamboo grades.

Results for PLA-miscanthus blends, in Table 2, showed a linear torque increase with fibre concentration in the compound. The more fibre added, the more torque needed and electricity consumed for the compound preparation. Blending PLA with miscanthus fibres also led to a pressure rise into the die (from 18 to 56 bars). As die geometry and temperature were kept constant, P_{mat} response must be linked to two different parameters, i.e. die filling degree and the compound viscosity. First, if feeding rate was kept constant, it was related to the matter weight (20 kg/h). Nevertheless, fibres and PLA have different densities, what could cause volume variations in the die depending on the fibre/polymer ratio. Natural fibre density is usually higher than PLA one (Nyambo et al., 2010) so adding more fibre should reduce matter volume. But a rod expansion was observed at the die exit and was a clue of trapped air into the blend while mixing was done. This caused volume increase in die and possibly higher pressure. Another parameter was the blend viscosity in the die. Therefore, the rheological behaviour of pellets produced was analysed to complete the observation made during compounding. These measurements showed an increasing relative melted viscosity from 0 to 40 wt% fibre loading (Fig. 3A). The composites rheological curves were fitted with the Oswald–De Waele power-law:

$$\eta = K\dot{\gamma}^{n-1},$$

where η is the viscosity (Pa s), $\dot{\gamma}$ is the shear rate (s^{-1}), K is the consistency (Pa s^n) and n is the power-law index. The coefficient of determination R^2 was around 0.99 for all the curves. The K values for the compounds with 0, 10, 20 and 40 wt% were 550, 1620, 5742 and 86 676 Pa, respectively. The n power-law index values were 0.57, 0.39, 0.21 and −0.24, respectively. In the latter case, a negative index was quite surprising but could be attributed to slip effects along the MiniLab walls (Fraiha et al., 2011). However, the rise of consistency value as the decrease of power-law index showed the difficulties for the blends to flow at high fibre concentrations. Indeed, fibres, that remained solid, were dispersed into molten polymer, hindering its flow and causing viscosity increase, especially in the low shear rate region (177–435 s^{-1}). These observations were coherent with previous works done in filled polymer systems (Kalaprasad et al., 2003; Guo et al., 2005). The orientation of the fibres, their interactions between each other such as their interactions with the matrix were possible viscosity increase causes. At low shear, fibres were disoriented and polymer chain entangled. Shear rate was insufficient to ensure the mobility of the system. Perturbations in normal flow resulted in viscosity increase. Fibre-to-fibre collisions and frictions in such disoriented system were more important. Kalaprasad et al. (2003) showed also that the more the affinity between the matrix and the polymer, the higher the blend viscosity. In the present case, the affinity between PLA and the fibres was low because no coupling was considered. Therefore, the influence of polymer–fibre interactions was likely lower than the ones of fibre disorientation and fibre-to-fibre collisions. At higher shear, fibres got oriented in the flow direction, the fibre-to-fibre collisions were diminished, and their impact on viscosity became lower. Thus, viscosity increase with fibre concentration most likely explained matter pressure and torque increases observed during compounding.

When the feeding rate was increased proportionally to screw speed at a set 20 wt% fibre loading, torque and matter pressure rose following the same trend: from 47.3 to 63.9% and from 30.3 to 37.5 bars, respectively (Fig. 4). By keeping Q/n ratio constant, global filling ratio (F_R) along the screws was kept constant too, as they were

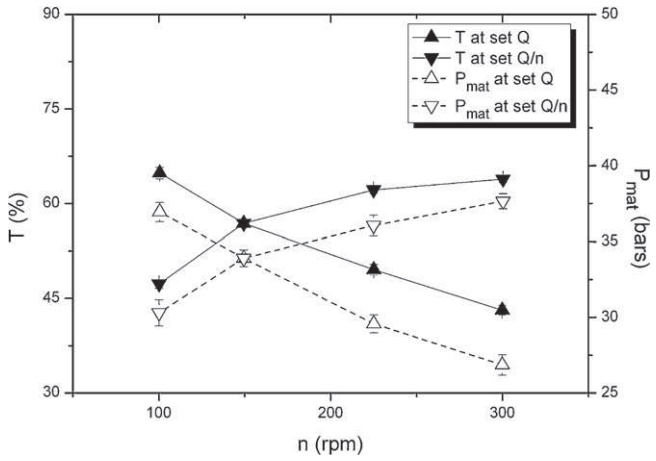

Fig. 4. Evolution of test torque (T) and matter pressure in the die (P_{mat}) with the screw speed (n) at set feeding rate (Q = 20 kg/h) and at set Q/n ratio (0.13 kg/h/rpm) for 20 wt% miscanthus filled compounds.

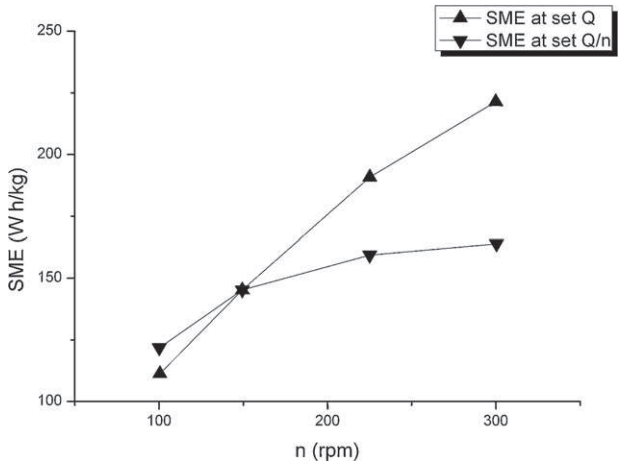

Fig. 5. Evolution of specific mechanical energy (SME) with the screw speed (n) at set feeding rate (Q = 20 kg/h) and at set Q/n ratio (0.13 kg/h/rpm) for 20 wt% miscanthus filled compounds.

linked by the relation $F_R = A \times (Q/n)$ (Vergnes et al., 1998), where A is a constant value depending on the extruder geometry and the screw profile that were kept the same for all the study. Actually, if the amount of matter introduced in the machine became bigger, it was compensated by lower residence time along the screws due to a faster screw rotation. Despite keeping a constant screw filling, a torque increase was observed as the screw speed increased. The die filling must be the cause. Indeed, even if filling was kept constant along the screws, more matter was passing through the die in the same period. As the flow rate of matter through the die increased, the pressure applied by the arriving matter on the matter already in the die became higher. Torque variations could be a repercussion of matter accumulation in the die, hindering screw rotation.

On the contrary, when the screw speed varied at the same feeding rate, Q/n ratio was either increased or reduced, and this tended to fill or to empty the screws, respectively. It can be seen in Fig. 4, for a set feeding rate, that both torque and matter pressure decreased when the screw speed increased: from 64.8 to 43.2% and from 36.9 to 26.9 bars, respectively. Additionally to global filling reduction by using higher screw speed, shear transferred to the matter got higher too. Thus, the matter in the extruder was fluidized, due to the PLA thermoplastic behaviour, and this could also explain the torque and matter pressure decreases.

In the point of view of electrical consumption, it can be seen in Fig. 5 that increasing the screw speed resulted in more energy spent. The torque reduction observed at a 20 kg/h feeding rate was not sufficient to compensate screw speed increase in the final SME calculation, and so the SME increased from 111 to 221 (W h)/kg. When Q/n ratio was kept constant, the SME logically rose in the same proportion than the torque (from 122 to 164 (W h)/kg), this one being the only parameter of SME calculation varying.

For the four bamboo grades reported in Table 2, no significant difference was observed on electrical consumption when compounded at 20 wt% loading (between 131 and 136 (W h)/kg for the SME value). Moreover, the energy needed for compounding bamboo fibres with PLA was lower than for miscanthus (145 (W h)/kg). In the case of miscanthus, matter pressure in the die was also higher than for bamboo grades while no differences were observed in rheological measurements between the fibres at 20 wt%. This observation could be linked to the self-heating of the matter in the die. Temperature in the die was set at 165 °C. However, real matter temperature measured in that zone was around 168 °C for miscanthus filled compound and around 170 °C for bamboo filled compounds. The difference in self-heating, that was a little higher with bamboo fibres, could come from difference in fibre abrasiveness, depending on its origin and chemical composition. Melt viscosity in the die was surely lower for the bamboo based blends with the highest measured temperature than with miscanthus based blends, what could explain the lower matter pressure and torque, and so the lower SME value, observed with bamboo compare to miscanthus. A slight increase in matter pressure (from 28 to 34 bars) was observed with decreasing fibre size at the entrance. At a 40 wt% loading, the feeder used in this study was limited to introduce enough bamboo fibres from B1 and B2 grades to reach a 20 kg/h total feeding rate. For B1, the reduction of feeding rate to 15 kg/h caused a decrease in torque (from 51% at 20 wt% loading and 20 kg/h feeding rate to 41% at 40 wt% loading and 15 kg/h feeding rate). The energy spent for the compounding was lower for B1 than for the three other grades prepared at the same 40 wt% loading: 140 (W h)/kg instead of at least 167 (W h)/kg. On the contrary, for B2 grade, where total feeding rate was even more reduced (12 kg/h), the torque reduction was in the same range than for B1 grade (from 53% at 20 wt% loading to 43% at 40 wt% loading). Consequently, the final energy spent was much higher (184 (W h)/kg). B3 and B4 bamboo grades and miscanthus were compounded in the same conditions for the two tested fibre loadings, i.e. at a 20 kg/h total feeding rate. Production of the 40 wt% B4 filled compound appeared to be instable with high variations of torque and die matter pressure. These variations did not come from the gravimetric feeder used, as an alert message is shown on the supervision as soon as the measured feeding rate drifted of 1% from the set value. No fibre accumulation was neither observed at the side feeder basis. The variations were possibly due to the very small fibre size, implying higher specific surface to wet by PLA and more difficulties to disperse the fibre in that case. These difficulties resulted in an inhomogeneous mixing. Melt polymer flow was probably perturbed by the presence of fibre agglomerates or partially wetted fibres, which had difficulties to get oriented in the flow direction. Indeed, most studies showed that at high fibre concentrations, interactions between fibres are more numerous. Interstitial spaces between the agglomerated fillers, containing immobilized polymer, can change system behaviour as if the filler concentration was actually higher than what had been added (Utracki and Fisa, 1982). Fig. 3B showed that B4 grade actually exhibited higher viscosity compare to the other grades. The viscosity increase probably explained the increased pressures in the die observed during extrusion with B4.

3.2. Fibre size

Process impact on the fibre size was evaluated by comparing miscanthus bundle length, diameter and aspect ratio distributions after the different steps of the process, i.e. extrusion, pelletizing and injection-moulding. As seen in Table 3, the main size reduction occurred in the extrusion part. Indeed, a 37% loss in fibre length and a 13% loss in fibre diameter were observed in 20 wt% filled compound rods. This resulted in an aspect ratio decrease (from 8.6 to 5.7). Pelletizing step caused a small decrease in length without affecting the diameter. This was due to fibre orientation in rod, mainly following the flow, and resulted in an additional aspect ratio loss (from 5.7 to 5.3) of low significance compare to the reduction after extrusion. Injection-moulding is a high-shear process but with low residence time compare to extrusion. It also affected fibre size. Both length and diameter were subjected to reduction in the same proportion: from 1.01 to 0.84 mm and from 0.21 to 0.17 mm, respectively. At the end, aspect ratio remained the same than in the pellets (5.2). Consequently, it appeared that twin-screw extrusion compounding was the process step causing the most fibre breakage, but also the most fibre separation from bundles.

Increasing the screw speed during compounding caused more shear to the matter in the screw restricted areas. Consequently, it was reasonable to think that the more shear provided, the more

Table 3
Miscanthus fibre size in extruded rods, pellets and injected materials.

	80/20 PLA/MIS composites			60/40 PLA/MIS composites		
	Length (mm)	Diameter (mm)	Aspect ratio	Length (mm)	Diameter (mm)	Aspect ratio
Extrusion	1.06 (0.59)	0.20 (0.12)	5.7 (2.3)	0.88 (0.43)	0.19 (0.10)	5.0 (2.0)
Pelletizing	1.01 (0.46)	0.21 (0.10)	5.3 (2.3)	0.83 (0.44)	0.17 (0.10)	5.1 (2.1)
Injection-moulding	0.84 (0.40)	0.17 (0.09)	5.2 (1.8)	0.78 (0.35)	0.17 (0.08)	4.8 (1.8)

Numbers in parentheses correspond to the standard deviations.

fibre breakage obtained. In fact, results of mean length and mean diameter in the final material revealed few variations in size in the case of 20 wt% miscanthus filled compounds obtained at set feeding rate and with screw speed from 100 to 300 rpm (Fig. 6). Distributions were very close to each other, and maximum fibre length and diameter (1.00 mm and 0.21 mm, respectively) were obtained with a 225 rpm screw speed. Mean aspect ratios were 4.9, 5.2, 5.1 and 5.4 for screw speeds of 100, 150, 225 and 300 rpm, respectively. When both feeding rate and screw speed increased, i.e. Q/n ratio kept constant, the same tendency was still observed in saving fibre length. At the same time, fibre diameter increased progressively but slightly with the screw speed (from 0.17 to 0.20 mm). Mean aspect ratios were 5.9, 5.2, 6.3 and 5.6, for feeding rates of 13, 20, 30 and 40 kg/h, respectively. For investigated compounding conditions, screw speed appeared to be insufficient neither to break fibres nor to separate bundles. By increasing screw speed, residence time into the extruder decreased, leading to more shear but on a shorter period. In addition, melted PLA was fluidized due to its shear-thinning behaviour, and so it had fewer difficulties to be conveyed through restricted areas along the twin-screw extruder. Wollerdorfer and Bader (1998) have shown that the matrix rheology had an impact on the final size distributions of flax fibres. When feeding rate was kept at 20 kg/h, by increasing the screw speed, the filling in mixing zone regions was reduced, what could also reduce their efficiency to transfer shear. In that case, a 0.09 kg/h/rpm Q/n ratio corresponding to a 225 rpm screw speed could be considered as an optimal condition to preserve fibre size. Despite these differences in length and diameter, in all cases, the fibre aspect ratio distributions in these compounds were found to be close to each other. These results went in the same way than Beaugrand and Berzin (2012) observations in PCL/hemp compounding by twin-screw extrusion, which enlightened also a small screw speed influence on fibre size.

Length and diameter for bamboo fibres in the final material are presented in Table 4. For 80/20 PLA/bamboo composites, the B1 grade that contained initially the longer and wider fibres also kept higher length and diameter after the global process, i.e. extrusion, pelletizing and injection-moulding, than the three other grades (B2 to B4). However, fibres from B1 grade were subjected to the greatest reduction in size as length loss was 72% instead of around 62% for B2 and B3 grades, and only 32% for B4 grade. Reduction in diameter was less important, between 25 and 35% for B1 to B3 grades and only 12% for B4 grade. The more important diameter loss for the B1 to B3 grades compare to B4 and miscanthus (−13%) was explained by SEM images presented in Fig. 1. Fibres were partly separated at the bundle ends in these three grades, what have surely eased fibre separation during process. Aspect ratios drastically decreased for the four bamboo grades, and particularly for B1 grade (−69%). At the end, gap between grades was dramatically reduced and differences in aspect ratios were found to be minor (from 4.8 to 5.6) compared to what they were before process (from 8.6 to 17.2). Few differences in size, between 80/20 and 60/40 PLA/bamboo composites, were observed for B3 and B4 grades. For B2 grade and more particularly for B1 grade, an extra size reduction was noticed in the injected material, especially for fibre length, as it was already observed for miscanthus (Table 3). B2 grade provided the longer fibres (0.74 mm), what could be explained by the use of a lower Q/n ratio (0.08 kg/h/rpm instead of 0.10 kg/h/rpm for B1 grade and 0.13 kg/h/rpm for B3 and B4 grades). Thus, as for miscanthus where a maximum in length was obtained for a 0.09 kg/h/rpm Q/n ratio, the Q/n ratio that gave the longer fibres for B2 bamboo grade was approximately the same (0.08 kg/h/rpm). Aspect ratio distributions are ranging from 4.5 to 5.6 (Table 4), what was close to the distributions obtained for the various PLA/miscanthus composites (ranging from 4.9 to 6.3). Analyses of mechanical and thermal properties will enlighten the influence of such size ranges on the composite properties.

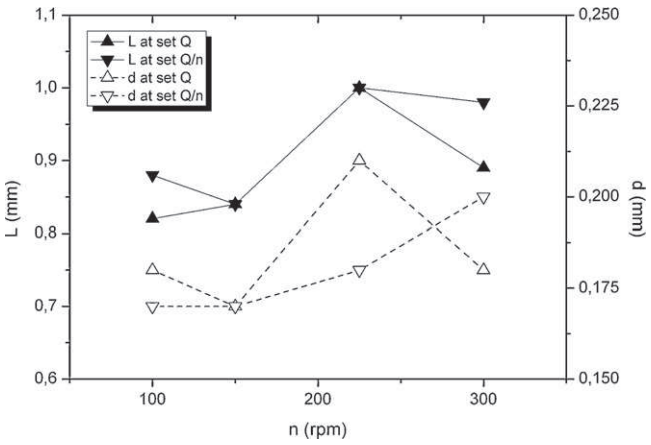

Fig. 6. Miscanthus fibre mean length (L) and mean diameter (d) in injected materials from 20 wt% filled compounds extruded at different screw speeds (n), at set feeding rate (Q = 20 kg/h) and at set Q/n ratio (0.13 kg/h/rpm).

3.3. Mechanical properties

Mechanical properties of the four bamboo composites were compared in Fig. 7 to miscanthus composites and PLA ones at the two different fibre loadings tested (20 and 40 wt%). For the five fibre types, important flexural and tensile modulus increases were observed by adding 20 and especially 40 wt% of natural fibres. Moreover, it appeared that B2 grade provided better increase at the two fibre concentrations for both flexural and tensile modulus. As an example, at 40 wt% B2 grade loading, flexural and tensile modulus increases were +164% and +197%, respectively, compare to neat PLA. On the other part, tensile strength was reduced for the five fibre types (up to −18% for 80/20 composites and up to −21% for 60/40 composites) as no specific treatment to improve fibre/polymer interface was made during this study. Nevertheless, less tensile strength reduction was observed with B2 grade: only −7% at both 20 wt% and 40 wt% fibre loading. For the five fibre types, the same reduction was observed for flexural strength at 20 wt% fibre loading. On the contrary, in the case of 60/40 composites, reduction in flexural strength was observed only with B3 and B4 grades, meaning that compounds filled with miscanthus or with B1 and B2 grades revealed flexural strengths higher than PLA one. Best flexural strength at 40 wt% fibre loading (80 MPa) was

Table 4
Bamboo fibre size in injected materials from B1 to B4 bamboo grades.

	80/20 PLA/bamboo composites			60/40 PLA/bamboo composites		
	Length (mm)	Diameter (mm)	Aspect ratio	Length (mm)	Diameter (mm)	Aspect ratio
B1	0.90 (0.45)	0.18 (0.11)	5.3 (2.1)	0.69 (0.42)	0.15 (0.08)	4.9 (1.7)
B2	0.80 (0.41)	0.15 (0.07)	5.6 (1.8)	0.74 (0.47)	0.15 (0.09)	5.0 (1.7)
B3	0.46 (0.25)	0.10 (0.05)	5.1 (2.2)	0.46 (0.23)	0.10 (0.05)	4.5 (1.6)
B4	0.33 (0.15)	0.07 (0.03)	4.8 (2.4)	0.31 (0.17)	0.06 (0.03)	5.4 (2.3)

Numbers in parentheses correspond to the standard deviations.

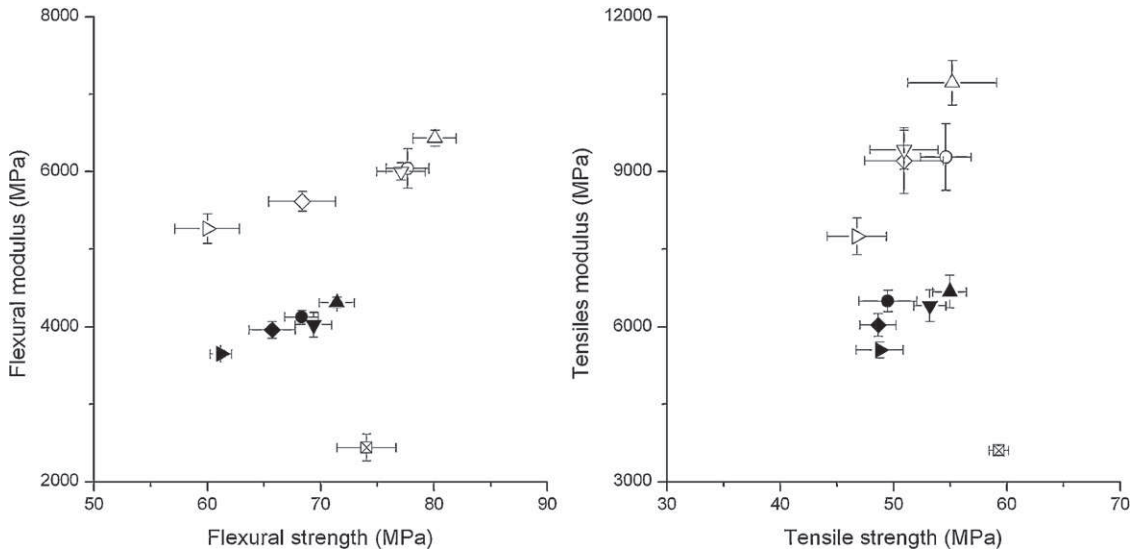

Fig. 7. Flexural and tensile properties for PLA (crossed square), 80/20 composites (filled symbol) and 60/40 composites (open symbol) filled with MIS (down triangle), B1 (circle), B2 (up triangle), B3 (diamond) and B4 (right triangle).

still obtained with B2 grade, and it was 8% more than PLA one. If 20 wt% loaded PLA/B2 grade compound performance in flexural and tensile strengths can be attributed to a higher aspect ratio (5.6 instead of 4.8–5.3 for the four other fibres), it was not the case for 40 wt% loaded one. For this concentration, B4 grade had the higher median aspect ratio (5.4 instead of 5.0 for B2 grade). Differences between aspect ratios for bamboo grades (Table 4) were in the same range of those observed between miscanthus composites, extruded with various screw speeds and various feeding rates (from 4.9 to 6.3). Consequently, the results of mechanical properties for these compounds were compared to estimate significance of aspect ratio influence on mechanical properties. Tensile properties results were chosen for such comparison.

Fig. 8 shows the tensile property variations for 20 wt% miscanthus filled compounds produced at different screw speeds. No significant difference was observed between these compounds, regarding to the standard deviations. As said previously, screw speed impact on fibre size was of low significance and variations observed at 225 rpm (Fig. 6) were not enough important to improve tensile properties. Modifying residence time of both fibre and PLA or providing more shear did not help improving the mixing between both components, as tensile strength remained quite the same for all the compounds tested. Beaugrand and Berzin (2012) also observed a small influence of screw speed on PCL/hemp composite mechanical properties. Contrarily to the observations in Fig. 5, feeding rate was found to have a more important role in their study on fibre size and composite mechanical properties. However, they used very low feeding rates (0.85 and 1.5 kg/h) compare to the range of feeding rate (from 13 to 40 kg/h) used here. It was believed that the quite higher residence time in their case caused a higher dependence of fibre size and composite properties to the feeding rate. If screw speed was found to have a little impact on properties, the compounds prepared at a 100 rpm screw speed exhibited very large standard deviations for tensile strength and tensile modulus compared to the others. This could be an evidence of an inhomogeneous mixing. At this screw speed, indeed, shear rate may not be sufficient to fluidize melt PLA enough for a good fibre dispersion or wettability. From these results, fibre aspect ratio may not be the parameter influencing the stiffness differences observed between the four bamboo grades.

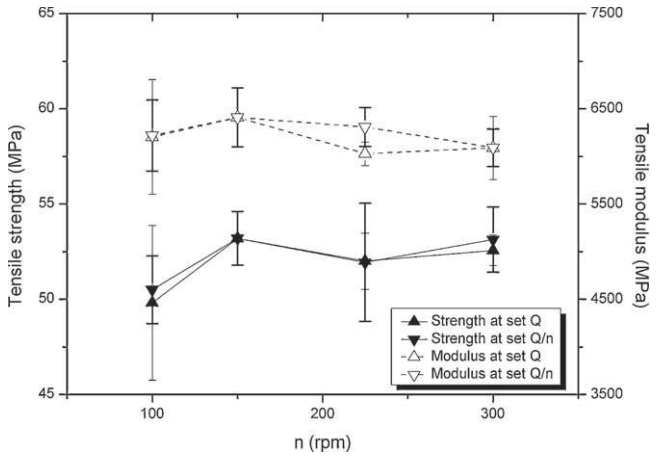

Fig. 8. Evolution of tensile strength and tensile modulus with the screw speed value (n) at set feeding rate (Q = 20 kg/h) and at set Q/n ratio (0.13 kg/h/rpm) for 20 wt% miscanthus filled compounds.

If aspect ratio variations between bamboo fibres were found to be negligible, variations in length and diameter were more important (Table 4). The longest fibres, i.e. B1 and B2 grades, reinforced the more PLA in flexural strength, even leading to its increase at a 40 wt% fibre loading as above mentioned. Diameter and particle shape most likely affected tensile and flexural strengths, and larger bundles observed for B1 and MIS fibres could explain worse performances for them than for B2 grade on the material strengthening (Fig. 7). Other parameters could have played a role such as the fibre dispersion, the fibre surface or its morphology. Chemical composition is also well known to influence intrinsic fibre properties and so, its reinforcement. Amount of cellulose is one important parameter. The more the cellulose in the fibre, the higher its intrinsic modulus and strength (Mohanty et al., 2000). The best mechanical properties were obtained from B1, B2 and MIS fibres (Fig. 7) which were richer in cellulose than other fibres (Table 1). On the other hand, B4 grade, which improved the less modulus and caused the more strength reduction for both mechanical tests, was also the bamboo grade containing the less cellulose. Concentration in hot water extractible components was also clearly higher in that grade (13 wt% of the dry matter instead of 5–7 wt% for the four other fibres). A previous study (Ashori and Nourbakhsh, 2010) reported better mechanical properties in PP/wood composites by removing these extractible components in oak and pine before compounding, confirming their negative effect on mechanical properties when present in the compound.

3.4. Thermal and thermo-mechanical properties

DSC thermograms revealed that incorporating miscanthus fibres in PLA using different fibre loadings and compounding conditions slightly increased its glass transition (T_g) and cold crystallization temperatures (T_{cc}): from 55.1 °C and 97.1 °C for neat PLA, respectively, to 56.3–58.0 °C and 97.8–101.8 °C for composites (Table 5). On the contrary, melting temperature (T_m) remained unchanged by the fibre presence. Changes in cold crystallization temperature up to almost 5 °C surely traduced more difficulties for the PLA chains to rearrange themselves in presence of miscanthus fibres. Indeed, a higher temperature meant that more energy was needed to initiate this rearrangement. Changes in chain mobility and initial PLA crystalline structure could be an explanation to these observations. Crystallinity rate after cooling was indeed found to be slightly increased in most cases (up to 10.9% instead of 9.1% for neat PLA) by the addition of fibres. However, in the case of 80/20 PLA/miscanthus composites, it was noticed that crystallinity rate was slightly reduced to 8.6–8.9% when a low screw speed (100 rpm) was used during twin-screw extrusion compounding. This is possibly due to an inhomogeneous fibre mixing and dispersion. Mathew et al. (2006) observed that fibres could promote crystallinity in PLA, crystallite growth being initiated at the fibre surface. An inhomogenous fibre dispersion and cluster formation reduced the specific fibre surface in contact with PLA, and so the areas where crystallites can be formed. Regarding to chain mobility, samples were analysed by DMA and thermograms revealed a height reduction of loss factor peak (Fig. 9). This phenomenon was imputed in previous works to a reduced chain mobility (Nyambo et al., 2010; Sreekumar et al., 2010) and resulted from the steric hindrance caused by fibre dispersion on polymer chain motion, as well as the slight crystallinity increase mentioned above. Indeed, mobility of polymer chain organized in crystallites was even more reduced. Consequently, cold

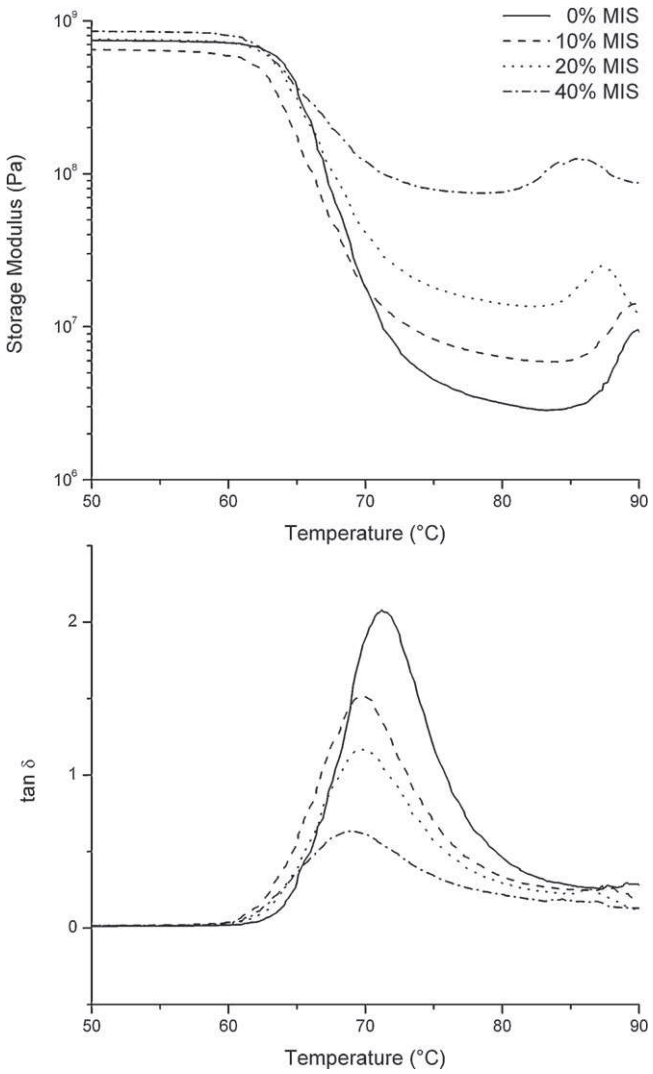

Fig. 9. Storage modulus and loss factor (tan δ) for neat PLA and PLA/miscanthus composites produced at a 20 kg/h feeding rate and a 150 rpm screw speed.

Table 5
DSC and heat deformation data for PLA/miscanthus composites.

Fibre loading	Q (kg/h)–n (rpm)	T_g (°C)	T_{cc} (°C)	T_m (°C)	χ (%)	Heat deformation (%)
Neat PLA	20–150	55.1	97.1	166.2	9.1	57.7 (3.1)
10 wt% MIS	20–150	56.3	97.8	166.4	10.2	51.0 (1.8)
20 wt% MIS	20–100	56.5	99.2	166.4	8.6	28.6 (2.2)
20 wt% MIS	20–150	56.9	99.6	165.9	10.4	34.2 (2.2)
20 wt% MIS	20–225	56.8	100.3	164.9	9.7	38.1 (2.9)
20 wt% MIS	20–300	56.9	101.8	166.4	9.4	37.5 (2.4)
20 wt% MIS	13–100	57.9	101.6	166.7	8.9	33.1 (2.8)
20 wt% MIS	30–225	57.0	101.1	166.3	10.9	35.4 (5.2)
20 wt% MIS	40–300	56.5	99.9	166.2	9.9	34.6 (0.7)
40 wt% MIS	20–150	58.0	99.3	166.7	10.2	7.8 (0.7)

Numbers in parentheses for heat deformation data correspond to the standard deviations.

Table 6
DSC and heat deformation data for PLA/bamboo composites produced at a 150 rpm screw speed.

Fibre loading[a]	T_g (°C)	T_{cc} (°C)	T_m (°C)	χ (%)	Heat deformation (%)
20 wt% B1	57.5	103.6	166.8	9.7	37.7 (3.2)
40 wt% B1	57.8	101.7	166.4	12.4	11.0 (1.2)
20 wt% B2	57.1	102.5	166.3	10.0	39.2 (5.8)
40 wt% B2	57.7	100.7	166.9	9.4	6.6 (0.4)
20 wt% B3	57.1	91.7	165.8	14.9	27.9 (1.2)
40 wt% B3	57.1	95.9	166.3	12.9	4.9 (1.2)
20 wt% B4	51.8	87.9	162.3	15.0	27.6 (3.2)
40 wt% B4	57.6	96.9	167.4	12.8	4.8 (0.2)

Numbers in parentheses for heat deformation data correspond to the standard deviations.
[a] Feeding rate was 12 kg/h for the 40 wt% B2 formulation, 15 kg/h for the 40 wt% B1 formulation, and 20 kg/h for all the others.

crystallization occurred at higher temperature. For glass transition, it was also shown in filled system that polymer modification at the matrix–filler interface caused free volume and chain mobility decrease resulting in glass transition temperature increase (Droste and Dibenedetto, 1969). It was seen on mechanical properties that interface interactions between the PLA and the natural fibres were weak. However, these weak interactions, the chain mobility reduction due to the fibre presence such as the crystallinity formation on the fibre surface could explain the observed T_g increase.

Another effect of the lowering of polymer chain mobility was the reduction of sample heat deformation: 58% without fibre addition, 51% at 10 wt% fibre loading, 29–38% at 20 wt% fibre loading, and only 8% at 40 wt% fibre loading (Table 5). The more fibre added, the more steric hindrance they caused, decreasing chain mobility and material deformation. Storage moduli in DMA (Fig. 9) were very close before PLA glass transition for all composites, its increase occurring only at 40 wt% of fibres compared to neat PLA. However, after glass transition, the storage modulus was found to remain higher along with the fibre concentration. Thus, it was concluded that 40 wt% filled material effectively enhanced PLA thermal stability by restraining polymer chain mobility. Less deformation was observed at 40 wt% fibre loading, and corresponding composite kept some stiffness after glass transition.

DSC results for bamboo grades are mentioned in Table 6. No differences were observed on transition temperature depending on the grade, except with 20 wt% B4 filled composite. For the B4 grade, glass transition and melting temperatures were reduced from 40 to 20 wt% fibre loading, what could be the clue of polymer chain reduction. Size-exclusion chromatography (SEC) measurements gave PLA weight average molar masses (M_w) of 18,800, 19,000, 18,800 and 18,400 g/mol for 20 wt% of B1, B2, B3 and B4 grades, respectively. The corresponding polydispersity indexes (I_p), representing the molecular weight distribution width, were 1.8, 2.4, 2.4 and 1.8, respectively. Thus, it was found no significant differences in PLA molar mass distributions in injected materials depending on the incorporated bamboo fibres. Reduction of PLA transition temperatures in the case of 20 wt% of B4 did not come from PLA molecular weight distribution, but might come from differences in the crystallization behaviour compare to the other composites. Indeed, the shortest fibres, from B3 and B4 grades, promoted PLA crystallization. Crystallinity rate was at least 12.8% for these two smallest grades instead of 9.4–12.4% for B1 and B2 grades. Tokoro et al. (2008) also observed this nucleating action of short bamboo fibre bundles in PLA. Defects due to fibre surface roughness can initiate crystal growth. Mathew et al. (2006) observed these differences of crystallinity promotion depending on the fibre surface topography. For B3 and B4 grades, crystallinity rate was higher at 20 wt% than at 40 wt% and reached 14.9 and 15.0% for the 80/20 PLA/B3 grade and PLA/B4 grade composites, respectively. At this amount, cold crystallization temperature was lower proving that PLA chain rearrangement was eased by nucleating effect of B3 and B4 as less energy was needed to initiate this rearrangement. With 40 wt%, it was thought that the too large amount of fibres curbed crystallite growth. At the same weight, smaller fibres represented more numerous particles than the longer ones, and so more specific surface in contact with the matrix, what caused more steric hindrance. There was a competition between fibre nucleating effect and hindrance of chain mobility, limiting the crystallite growth. This competition between the filler nucleating effect and its impeding effect on crystallization at high loading was also observed in PLA filled with clay by Wu et al. (2007).

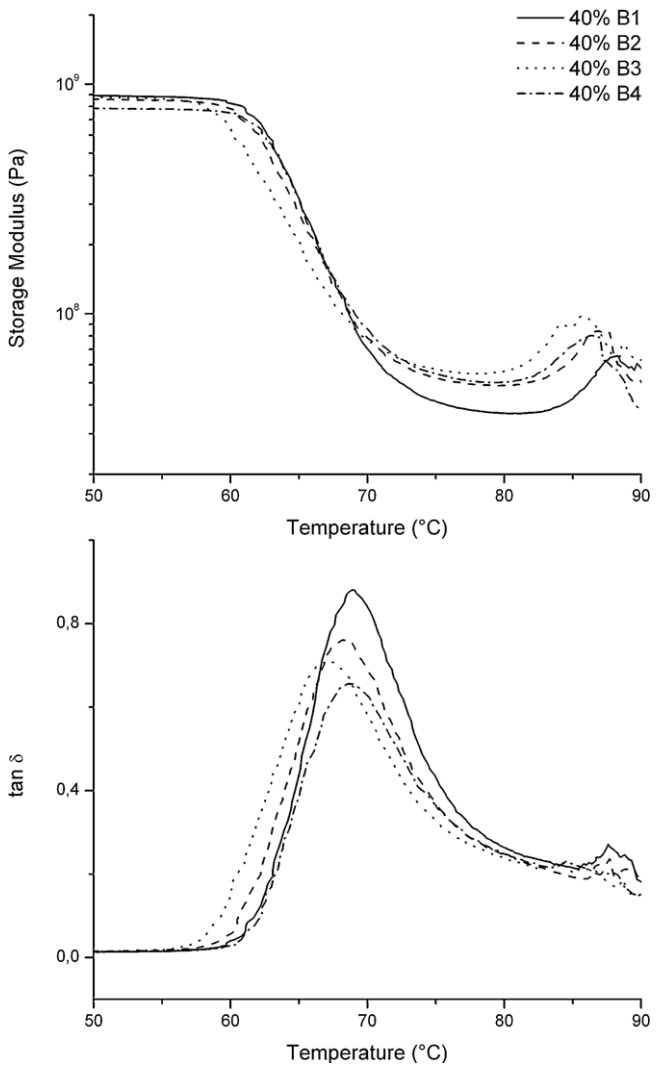

Fig. 10. Storage modulus and loss factor (tan δ) for 60/40 PLA/bamboo composites produced at a 150 rpm screw speed (total feeding rate was 12 kg/h for B2 grade, 15 kg/h for B1 grade, and 20 kg/h for B3 and B4 grades).

Decrease in polymer chain mobility with the shortest bamboo fibres, due to the promotion of PLA crystallinity and the steric hindrance of more numerous particles, was confirmed by DMA results (Fig. 10). For these grades, the height of loss factor peak was the lowest. Consequently, fibre size in final material, reported in Table 4, played a role on composite heat deformation (Table 6) by reducing polymer chain mobility. Indeed, best thermal stabilities were obtained from B3 and B4 grades, especially with a 40 wt% fibre loading: 4.9 and 4.8% for heat deformation, respectively. DMA profiles of 60/40 PLA/bamboo composites reported in Fig. 10 also showed an advantage of B3 and B4 shorter grades on the storage modulus after glass transition. These observations are confirmed in the heat deformation results of 80/20 PLA/miscanthus compounds produced at a 20 kg/h feeding rate (Table 5). Heat deformation was found to be higher for compounds extruded at high screw speeds (225 and 300 rpm, respectively), i.e. with lower Q/n ratios (0.09 and 0.07 kg/h/rpm, respectively). These compounds contained longer and larger fibres in the final material, especially the one produced at a 225 rpm screw speed (Fig. 6).

It can be concluded from these results that material thermal stability is improved by reducing the polymer chain mobility. This effect was obtained with high fibre concentrations and with the use of small fibres, which both restricted polymer chain motion by steric impeding and crystallinity promotion.

4. Conclusion

Miscanthus fibre and bamboo fibre reinforced PLA composites were prepared by twin-screw extrusion. Influence of compounding parameters such as screw speed and feeding rate on fibre morphology and final materials properties were evaluated. Increasing the screw speed, and so the shear rate into the blend, as increasing the feeding rate helped to save fibre bundle length, what was attributed to a lower residence time in the machine and a reduced blend viscosity. However, the differences in fibre morphology inside the injected materials were not enough important to see differences in their mechanical properties. Composite heat stability was better for compounds extruded at lower screw speed for which less mechanical energy was spent. Using 150 rpm screw speed was the best choice for energy saving as 100 rpm was insufficient to have homogenous properties.

The bamboo grade study with four distinct initial size distributions showed that the longer the fibres were before the process, the more they were broken. On the mechanical property point of view, longer fibres would be preferred as they reinforced the material the most, especially in flexural solicitation. Dispersing numerous short fibres improved thermo-mechanical properties and reduced the material heat deformation, as these fibres promoted PLA crystallinity and restrained polymer chain mobility.

Acknowledgements

We would like to thank the French Environment and Energy Management Agency (ADEME) and the "Conseil Général des Hautes-Pyrénées" which have participated to this work via financial support, as well as Nathalie Aubazac and Joël Alexis (LGP) for their help for SEM images.

References

Ashori, A., Nourbakhsh, A., 2010. Reinforced polypropylene composites: effects of chemical compositions and particle size. Bioresour. Technol. 101, 2515–2519.

Beaugrand, J., Berzin, F., 2012. Lignocellulosic fiber reinforced composites: influence of compounding conditions on defibrization and mechanical properties. J. Appl. Polym. Sci., http://dx.doi.org/10.1002/app.38468.

Bledzki, A.K., Letman, M., Viksne, A., Rence, L., 2005. A comparison of compounding processes and wood type for wood fibre—PP composites. Composites: Part A 36, 789–797.

Bourmaud, A., Pimbert, S., 2008. Investigations on mechanical properties of poly(propylene) and poly(lactic acid) reinforced by miscanthus fibers. Composites: Part A 39, 1444–1454.

Droste, D.H., Dibenedetto, A.T., 1969. The glass transition temperature of filled polymers and its effect on their physical properties. J. Appl. Polym. Sci. 13, 2149–2168.

Faruk, O., Bledzki, A.K., Fink, H.-P., Sain, M., 2012. Biocomposites reinforced with natural fibers: 2000–2010. Prog. Polym. Sci., http://dx.doi.org/10.1016/j.progpolymsci.2012.04.003.

Fischer, E.W., Sterzel, H.J., Wegner, G., 1973. Investigation of the structure of solution grown crystals of lactide copolymers by means of chemical reactions. Kolloid-Z. Z. Polym. 251, 980–990.

Fraiha, M., Biagi, J.D., Ferraz, A.C. de O., 2011. Rheological behavior of corn and soy mix as feed ingredients. Ciênc. Tecnol. Aliment. 31, 129–134 (Online).

Guo, R., Azaiez, J., Bellehumeur, C., 2005. Rheology of fiber filled polymer melts: role of fiber–fiber interactions and polymer–fiber coupling. Polym. Eng. Sci. 45, 385–399.

Hong, C., Fang, J., Jin, A., Cai, J., Guo, H., Ren, J., Shao, Q., Zheng, B., 2011. Comparative growth, biomass production and fuel properties among different perennial plants, bamboo and miscanthus. Bot. Rev. 77, 197–207.

Huda, M.S., Drzal, L.T., Misra, M., Mohanty, A.K., 2006. Wood-fiber-reinforced poly(lactic acid) composites: evaluation of the physicomechanical and morphological properties. J. Appl. Polym. Sci. 102, 4856–4869.

Jamshidian, M., Tehrany, E.A., Imran, M., Jacquot, M., Desobry, S., 2010. Poly-lactic acid: production, applications, nanocomposites, and release studies. Compr. Rev. Food Sci. Food Saf. 9, 552–571.

Johnson, M., Tucker, N., Barnes, S., Kirwan, K., 2005. Improvement of the impact performance of a starch based biopolymer via the incorporation of *Miscanthus giganteus* fibres. Ind. Crop. Prod. 22, 175–186.

Joseph, P.V., Joseph, K., Thomas, S., 1999. Effect of processing variables on the mechanical properties of sisal-fiber-reinforced polypropylene composites. Compos. Sci. Technol. 59, 1625–1640.

Kalaprasad, G., Mathew, G., Pavithran, C., Thomas, S., 2003. Melt rheological behavior of intimately mixed short sisal-glass hybrid fiber-reinforced low-density polyethylene composites. I. Untreated fibers. J. Appl. Polym. Sci. 89, 432–442.

Kymäläinen, H.R., Sjöberg, A.M., 2008. Flax and hemp fibres as raw materials for thermal insulations. Build. Environ. 43, 1261–1269.

Le Duc, A., Vergnes, B., Budtova, T., 2011. Polypropylene/natural fibres composites: analysis of fibre dimensions after compounding and observations of fibre rupture by rheo-optics. Composites: Part A 42, 1727–1737.

Le Moigne, N., van den Oever, M., Budtova, T., 2011. A statistical analysis of fibre size and shape distribution after compounding in composites reinforced by natural fibres. Composites: Part A 42, 1542–1550.

Lezak, E., Kulinski, Z., Masirek, R., Piorkowska, E., Pracella, M., Gadzinowska, K., 2008. Mechanical and thermal properties of green polylactide composites with natural fillers. Macromol. Biosci. 8, 1190–1200.

Masirek, R., Kulinski, Z., Chionna, D., Piorkowska, E., Pracella, M., 2007. Composites of poly(L-lactide) with hemp fibers: morphology and thermal and mechanical properties. J. Appl. Polym. Sci. 105, 255–268.

Mathew, A.P., Oksman, K., Sain, M., 2006. The effect of morphology and chemical characteristics of cellulose reinforcements on the crystallinity of polylactic acid. J. Appl. Polym. Sci. 101, 300–310.

Mohanty, A.K., Misra, M., Hinrichsen, G., 2000. Biofibres, biodegradable polymers and biocomposites: an overview. Macromol. Mater. Eng. 276–277, 1–24.

Nyambo, C., Mohanty, A.K., Misra, M., 2010. Polylactide-based renewable green composites from agricultural residues and their hybrids. Biomacromolecules 11, 1654–1660.

Ogbomo, S.M., Chapman, K., Webber, C., Bledsoe, R., D'Souza, N.A., 2009. Benefits of low kenaf loading in biobased composites of poly(L-lactide) and kenaf fiber. J. Appl. Polym. Sci. 112, 1294–1301.

Oksman, K., Skrifvars, M., Selin, J.-F., 2003. Natural fibres as reinforcement in polylactic acid (PLA) composites. Compos. Sci. Technol. 63, 1317–1324.

Oksman, K., Mathew, A.P., Långström, R., Nyström, B., Joseph, K., 2009. The influence of fibre microstructure on fibre breakage and mechanical properties of natural fibre reinforced polypropylene. Compos. Sci. Technol. 69, 1847–1853.

Okubo, K., Fujii, T., Yamamoto, Y., 2004. Development of bamboo-based polymer composites and their mechanical properties. Composites: Part A 35, 377–383.

Plackett, D., 2004. Maleated polylactide as an interfacial compatibilizer in biocomposites. J. Polym. Environ. 12, 131–138.

Sreekumar, P.A., Gopalakrishnan, P., Leblanc, N., Saiter, J.M., 2010. Effect of glycerol and short sisal fibers on the viscoelastic behavior of wheat flour based thermoplastic. Composites: Part A 41, 991–996.

Sykacek, E., Schlager, W., Mundigler, N., 2010. Compatibility of softwood flour and commercial biopolymers in injection molding. Polym. Compos. 31, 443–451.

Tokoro, R., Vu, D., Okubo, K., Tanaka, T., Fujii, T., Fujiura, T., 2008. How to improve mechanical properties of polylactic acid with bamboo fibers. J. Mater. Sci. 43, 775–787.

Tuominen, J., Kylmä, J., Kapanen, A., Venelampi, O., Itävaara, M., Seppälä, J., 2002. Biodegradation of lactic acid based polymers under controlled composting conditions and evaluation of the ecotoxicological impact. Biomacromolecules 3, 445–455.

Utracki, L.A., Fisa, B., 1982. Rheology of fiber- or flake-filled plastics. Polym. Compos. 3, 193–211.

Van Hulle, S., Roldán-Ruiz, I., Bockstaele, E., Muylle, H., 2010. Comparison of different low-input lignocellulosic crops as feedstock for bio-ethanol production. In: Huyghe, C. (Ed.), Sustainable Use of Genetic Diversity in Forage and Turf Breeding. Springer Netherlands, Dordrecht, pp. 365–368.
Van Soest, P.J., Wine, R.H., 1967. Use of detergents in the analysis of fibrious feeds. IV. Determination of plant cell wall constituents. J. Assoc. Off. Anal. Chem. 50, 50–55.
Van Soest, P.J., Wine, R.H., 1968. Determination of lignin and cellulose in acid detergent fiber with permanganate. J. Assoc. Off. Anal. Chem. 51, 780–785.
Vergnes, B., Della Valle, G., Delamare, L., 1998. A global computer software for polymer flows in corotating twin screw extruders. Polym. Eng. Sci. 38, 1781–1792.
Wollerdorfer, M., Bader, H., 1998. Influence of natural fibres on the mechanical properties of biodegradable polymers. Ind. Crop. Prod. 8, 105–112.
Wu, D., Wu, L., Wu, L., Xu, B., Zhang, Y., Zhang, M., 2007. Nonisothermal cold crystallization behavior and kinetics of polylactide/clay nanocomposites. J. Polym. Sci. B: Polym. Phys. 45, 1100–1113.